

Making the decoy-state measurement-device-independent quantum key distribution practically useful

Yi-Heng Zhou^{1,2}, Zong-Wen Yu^{1,3}, and Xiang-Bin Wang^{1,2,4*}

¹State Key Laboratory of Low Dimensional Quantum Physics, Department of Physics, Tsinghua University, Beijing 100084, Peoples Republic of China

²Synergetic Innovation Center of Quantum Information and Quantum Physics, University of Science and Technology of China Hefei, Anhui 230026, China

³Data Communication Science and Technology Research Institute, Beijing 100191, China

⁴Jinan Institute of Quantum technology, SAICT, Jinan 250101, Peoples Republic of China

The relatively low key rate seems to be the major barrier to its practical use for the decoy state measurement device independent quantum key distribution (MDIQKD). We present a 4-intensity protocol for the decoy-state MDIQKD that hugely raises the key rate, especially in the case the total data size is not large. Also, calculation shows that our method makes it possible for secure private communication with *fresh* keys generated from MDIQKD with a delay time of only a few seconds.

PACS numbers: 03.67.Dd, 42.81.Gs, 03.67.Hk

I. INTRODUCTION

One of the most important expected advantage for Quantum key distribution (QKD)[1, 2] is to generate fresh secure keys for instant use, so as to achieve a higher-level security in private communications. This demands a considerably final key generation rate in a time scale of seconds. The existing technologies can achieve such a goal if the decoy-state BB84 is applied [3–14]. For example, given the system repetition rate of 1 GHz[15], one can make a key rate much higher than the standard of GSM(the Global system for mobile communication), 13K bits per second (bps), at a rather long distance such as 50 km. This method can keep the unconditional security of QKD with an imperfect single-photon source [16, 17]. However, to patch up the security loophole caused by the limited detection efficiency (including channel loss) [18], one has to seek other methods such as the so called device independent QKD (DI-QKD) [19] and the measurement-device independent QKD (MDI-QKD) which was based on the idea of entanglement swapping [20, 21]. By using the decoy-state method, Alice and Bob can use imperfect single-photon sources [21, 22] securely in the MDI-QKD. The decoy-state MDI-QKD has the advantage of getting rid of all detector side-channel attacks with imperfect single-photon sources. The method has been studied extensively both experimentally [23–28] and theoretically [22, 29–39].

However, the key rate of the decoy-state MDIQKD is rather low, e.g., in the well known Hefei experiment[28], it is 0.018 bps over 200 km, with the set up running for 130 hours. The low key rate seems to be the only barrier

to its final practical use. On the other hand, prior art results show that, if the statistical fluctuation is taken into consideration, we need a large data size so as to reach a considerable final key rate[29, 30, 32, 38]. In particular, the number of total pulses at each side N_t is assumed to be larger than 10^{12} . It seems to be rather challenging a task to reach a considerable key rate with a small data size, such as $N_t \sim 10^9 - 10^{10}$, which can be done in a time scale of 1 second or a few seconds, given the set-up repetition rate of GHz level[15, 40]. Note that none of the prior art works can generate a final key in a considerable key rate given a small data size such as $N_t \sim 10^9 - 10^{10}$.

Here we present a method that can produce a key rate much higher than any existing theoretical or experimental results and can generate considerable key rate in a very short time. Calculation shows that our method can be applied for *fresh* key generation with decoy-state MDI-QKD, given the GHz-level set-up repetition rate.

In what follows, we shall first review the decoy-state MDI-QKD and our protocol in section II. We then take the improved analysis in section III. There we show a very tricky result that the lower bound of the averaged value of yield and the upper bound phase-flip error rate of all single-photon pairs in both bases can be estimated tightly with observed data in X basis only. Based on this fact, we show with explicit formulas that instead of taking the worst-case estimations for the yield and phase-flip error rate of single-photon pairs separately, we can treat them jointly pointing directly to the worst-case result of the final key rate. We then present the numerical simulation results in section IV. The results there show huge advantages of this work in the key rates. The article is ended with a concluding remark.

*Email Address: xbwang@mail.tsinghua.edu.cn

[†]Also a member of Center for Atomic and Molecular Nanosciences at Tsinghua University

II. PROTOCOL

We use subscript A or B to denote a source at Alice's side or Bob's side. In our protocol, sources x_A and y_A (x_B and y_B) only emit pulses in X basis while source z_A (z_B) only emits pulses in Z basis. The protocol needs four different states $\rho_{o_A} = |0\rangle\langle 0|$, ρ_{x_A} , ρ_{y_A} , ρ_{z_A} ($\rho_{o_B} = |0\rangle\langle 0|$, ρ_{x_B} , ρ_{y_B} , ρ_{z_B}) respectively.

In photon number space, suppose

$$\rho_{x_A} = \sum_k a_k |k\rangle\langle k|, \quad \rho_{x_B} = \sum_k b_k |k\rangle\langle k|, \quad (1)$$

$$\rho_{y_A} = \sum_k a'_k |k\rangle\langle k|, \quad \rho_{y_B} = \sum_k b'_k |k\rangle\langle k|, \quad (2)$$

$$\rho_{z_A} = \sum_k a''_k |k\rangle\langle k|, \quad \rho_{z_B} = \sum_k b''_k |k\rangle\langle k|, \quad (3)$$

We call x_A , x_B as well as y_A , y_B the decoy sources; z_A , z_B the signal sources, and o_A , o_B the vacuum sources.

At each time, Alice will randomly choose source l_A with probability p_{l_A} for $l = o, x, y, z$. Similarly, Bob will randomly choose source r_B with probability p_{r_B} for $r = o, x, y, z$. The emitted pulse pairs (one pulse from Alice, one pulse from Bob) are sent to the un-trusted third party (UTP). We shall use notation lr to indicate the two-pulse source when Alice use source l_A and Bob use source r_B to general a pulse pair, e.g., source xy is the source that Alice uses source x_A and Bob uses source y_B . Also, here in our protocol, the intensity for pulses in Z basis can be different from those of X basis, this makes more freedom in choosing the intensities and hence further raises the key rate. Those effective events caused by pulse pairs from source zz will be used for key distillation, while the effective events caused by sources in X basis and vacuum sources will be used to estimate the yield and the phase-flip error rate of the single-photon pulse pairs.

III. IMPROVED ANALYSIS FOR FINAL KEY RATE

We need lower bound value for s_{11}^Z , the yield of single-photon pulse pairs in Z basis. However, as discussed by [32, 38], since in actual applications, the number of pulse pairs in Z is much larger than the number of pulse pairs in X basis, we can use the lower bound of the averaged values of the yield of single-photon pairs in *all* bases for the quantity in Z basis only. A very tricky point here is that we can tightly lower bound the yield of *all* single photon pairs using the observed data in X -basis only.

A. Theorems for statistical fluctuation

We define the counting rate (yield) of pulses of a certain set \mathcal{C} as

$$S_{\mathcal{C}} = \frac{n_{\mathcal{C}}}{N_{\mathcal{C}}} \quad (4)$$

where $n_{\mathcal{C}}$ is the number of valid counts due to pulses in \mathcal{C} , and $N_{\mathcal{C}}$ is the number of pulses in set \mathcal{C} . Actually, in MDI-QKD, we always use pulses pairs from Alice and Bob. So, more strictly speaking, "pulses" above are actually "pulse pairs". Given this definition, we have the following theorem:

Theorem 1: Suppose set $\mathcal{M} = \{\mathcal{M}_1, \mathcal{M}_2, \dots, \mathcal{M}_i, \dots, \mathcal{M}_K\}$ with $K \geq 1$, and any subset \mathcal{M}_i contains $N_{\mathcal{M}_i}$ pulse pairs. Set $\mathcal{L} = \{\mathcal{L}_1, \mathcal{L}_2, \dots, \mathcal{L}_i, \dots, \mathcal{L}_K\}$. Define quantity $\langle S_{\mathcal{M}} \rangle_{\mathcal{L}} = \sum_{i=1}^K c_i S_{\mathcal{L}_i}$ with $c_i = \frac{N_{\mathcal{M}_i}}{N_{\mathcal{M}}}$. The following inequality holds with a probability larger than $1 - \epsilon$:

$$-\Delta_- \leq S_{\mathcal{M}} - \langle S_{\mathcal{M}} \rangle_{\mathcal{L}} \leq \Delta_+ \quad (5)$$

provided that the following conditions hold for any i :

i) Set \mathcal{M}_i is a random subset of \mathcal{L}_i , i.e., all elements in set \mathcal{L}_i have equal probability to be also an element of set \mathcal{M}_i ; $\mathcal{M}_i \cap \mathcal{M}_j = \emptyset$, $\mathcal{L}_i \cap \mathcal{L}_j = \emptyset$ for $i \neq j$ where \emptyset is the empty set;

ii) All elements in \mathcal{L}_i are independent and identical.

As shown in [28, 32], the values Δ_+ , Δ_- can be determined explicitly by using Chernoff bound given the failure probability ϵ . Though contents of theorem above have been studied and applied elsewhere [14, 32, 38], we believe that the theorem presented here offers a clearer picture for study of statistical fluctuation in the decoy-state MDI-QKD. In particular, in considering the averaged value of yield and phase-flip error rate of the single-photon pairs, we don't have to limit them to the average over a certain basis, as was so in Ref. [32, 38, 39]. With our theorem 1, we can use the average over pulses in *different* bases. As demonstrated later in this article, this theorem can help us do calculations more efficiently, e.g., our theorem 2 and theorem 3. Obviously, this theorem also holds for the error yields, and hence for the phase-flip error of single-photon pairs, as shall be studied latter.

Theorem 1 shall also apply for the conventional BB84 QKD by just regarding elements of any set there as a single pulse. Here in our application for MDI-QKD, \mathcal{L} shall be a set that contains pulse pairs from several real two-pulse sources. We shall regard pulse pairs of a specific two-mode Fock state from \mathcal{L} as a set \mathcal{L}_i . Therefore in applying Theorem 1 later in this paper, we shall substitute subscript i by double subscript mn in Theorem 1 and \mathcal{L}_{mn} is a set that contains all pulse pairs of state $|m\rangle\langle m| \otimes |n\rangle\langle n|$ from \mathcal{L} . Before any further investigation, we list the following simplified mathematical notations first.

(1) \mathcal{C}^{lr} : the set for all pulse pairs from source lr ; (Sometimes we simply use notation lr for \mathcal{C}^{lr} , if this does not cause any confusion.)

(2) \mathcal{C}_{mn} : the set of pulse pairs of state $|m\rangle\langle m| \otimes |n\rangle\langle n|$ from set \mathcal{C} . For example, \mathcal{C}_{mn}^{lr} and \mathcal{L}_{mn} are sets for pulse pairs of state $|m\rangle\langle m| \otimes |n\rangle\langle n|$ from sets \mathcal{C}^{lr} and \mathcal{L} , respectively.

(3) s_{mn}^{lr} : yield of set \mathcal{C}_{mn}^{lr} , i.e., $s_{mn}^{lr} = S_{\mathcal{C}_{mn}^{lr}}$.

(4) $s_{mn}^{\mathcal{L}}$: yield of set \mathcal{L}_{mn} , i.e., $s_{mn}^{\mathcal{L}} = S_{\mathcal{L}_{mn}}$.

(5) S_{lr} : yield of source lr , i.e. $S_{\mathcal{C}^{lr}}$.

In any real experimental set-up, the total pulses sent by both sides are finite. In order to extract the secure final key, the effect of statistical fluctuations caused by the finite-size key must be considered. In this case, in general

$$s_{mn}^{lr} \neq s_{mn}^{l'r'} \quad (6)$$

if $l'r' \neq lr$. In this case, to obtain the lower bound value for s_{11} (yield of single-photon pairs) and upper bound value of e_{11}^{ph} (phase-flip rate of single-photon pairs), one can apply theorem 1 to a suitably chosen set of two pulse sources, \mathcal{D} . As an example we choose[41]

$$\mathcal{D} = \{oo, ox, xo, oy, yo, xx, yy\}. \quad (7)$$

To apply our theorem, we also need to choose set \mathcal{L} . First, we use

$$\mathcal{L} = \mathcal{D}. \quad (8)$$

We can write the density matrix of any two-pulse source $lr \in \mathcal{D}$ in the following form

$$\rho_{lr} = \sum_{m,n} c_{mn}^{lr} |m\rangle\langle m| \otimes |n\rangle\langle n|. \quad (9)$$

Relating this, we now *define* $\langle S_{lr} \rangle_{\mathcal{L}}$ as

$$\langle S_{lr} \rangle_{\mathcal{L}} = \sum_{m,n} c_{mn}^{lr} s_{mn}^{\mathcal{L}}. \quad (10)$$

According to this equation, we can list many equations (constraints) and hence calculate the lower bound of $s_{11}^{\mathcal{L}}$ either by formula or by linear programming, as shown in details in the Appendix. Therefore we have the following theorem:

Theorem 2: In the non-asymptotic case, using the observed data (number of counts) of pulses in X basis and pulses from vacuum sources, e.g., pulse pairs from set \mathcal{D} , we can lower bound the yield of single-photon pairs in X basis, the yield of all single photon pairs in both bases, and also the yield of those single photon pairs in Z basis only.

In the Appendix we shall show the explicit formula for lower bound the yield of single-photon pairs in X basis by Eq.(22), and the yield of all single-photon pairs in both X basis and Z basis by Eq.(27). In particular, the lower bound of the yield of the single-photon pairs is a functional of \mathcal{H} and

$$\mathcal{H} = a_0 \langle S_{ox} \rangle_{\mathcal{L}} + b_0 \langle S_{xo} \rangle_{\mathcal{L}} - a_0 b_0 \langle S_{oo} \rangle_{\mathcal{L}}. \quad (11)$$

Given theorem 2, we can actually deduce the lower bound of yield of single-photon pairs in Z basis through using the observed data in X basis only, even for the non-asymptotic calculation. *This makes it possible to treat the yield of single-photon pairs and the phase-flip error of single-photon pairs jointly* as shown below because both of them are dependent on the same quantity \mathcal{H} . We shall take a detailed study on this very important point below.

B. Joint study for worst-case result of key rate

We denote $\underline{s}_{11}(\mathcal{H})$ as the lower bound of $s_{11}^{\mathcal{L}}$ with a given value \mathcal{H} . Note that \mathcal{H} is defined by Eq.(11). The value $\underline{s}_{11}(\mathcal{H})$ can be calculated rather tightly if we use constraints in Eq.(23). As shown in the Appendix, the value $\underline{s}_{11}(\mathcal{H})$ calculated by these constraints can also lower bound $s_{11}^{\mathcal{L}'}$, the yield of all single-photon pairs because there is a same set of constraints for quantities $\langle S_{lr} \rangle_{\mathcal{L}'}$, as given by Eqs.(28,24). Here $\mathcal{L}' = \mathcal{D} \cup \mathcal{C}_{11}^{zz}$. Therefore we shall simply use one notation $\underline{s}_{11}(\mathcal{H})$ for both the lower bound of $s_{11}^{\mathcal{L}}$ and the lower bound of $s_{11}^{\mathcal{L}'}$, given \mathcal{H} . Actually, using the method in Ref.[39], the functional $\underline{s}_{11}(\mathcal{H})$ can be analytically formulated.

Second, we can also formulate the phase-flip error rate of single-photon pairs for all single-photon pairs[32, 38, 39]. We regard this as a functional of \mathcal{H} . As its original definition in the Pauli channel model[42, 43], a phase

flip error is a $\sigma_z = \begin{pmatrix} 1 & 0 \\ 0 & -1 \end{pmatrix}$ error that takes a phase

shift in Z basis. We adopt this definition for all qubits in both X -basis and Z -basis. The σ_z errors on qubits in Z -basis are not physically detectable, but they do exist. The σ_z error on qubits in X basis can be detected, it is just the flipping error in the basis. We can deduce the σ_z error rate of all single-photon pairs through measuring the σ_z error on those single-photon pairs in X basis only.

Denote the σ_z -error yield of any set \mathcal{C} by $T_{\mathcal{C}}$, we have $T_{\mathcal{C}} = \frac{\tilde{n}_{\mathcal{C}}}{N_{\mathcal{C}}}$, and $\tilde{n}_{\mathcal{C}}$ is the number or error bits due to set \mathcal{C} . Denoting $T_{xx} = T_{\mathcal{C}^{xx}}$ we have

$$T_{xx} = \sum_{m,n} c_{mn}^{xx} T_{mn}^{xx} \quad (12)$$

where T_{mn}^{xx} is error yield of set \mathcal{C}_{mn}^{xx} . Taking the same definition of set \mathcal{L}' as used earlier, we *define* quantity $\langle T_{xx} \rangle_{\mathcal{L}'}$ as

$$\langle T_{xx} \rangle_{\mathcal{L}'} = \sum_{m,n} c_{mn}^{xx} T_{mn}^{\mathcal{L}'}. \quad (13)$$

We can now apply our theorem 1 to make a non-trivial treatment for error yield and bound the phase-flip error *all* single-photon pairs in both bases.

$$e_{11}^{\mathcal{L}'} \leq \bar{e}_{11}^{ph} = \frac{\xi}{a_1 b_1 \underline{s}_{11}}, \quad (14)$$

and $\xi = \langle T_{xx} \rangle_{\mathcal{L}'} - a_0 \langle T_{ox} \rangle_{\mathcal{L}'} - b_0 \langle T_{xo} \rangle_{\mathcal{L}'} + a_0 b_0 \langle T_{oo} \rangle_{\mathcal{L}'}$. This gives the phase flip error for all single-photon pairs by using observed data of source xx only. To a good approximation, this is also the phase-flip error rate of single-photon pairs in Z -basis only, because almost all single-photon pairs are from source zz .

Theorem 3 Applying our theorem 1, together with Eq.(14) one can obtain the upper bound of the phase-flip error rate (σ_z -error rate) for all single-photon pairs by using observed data of source xx only.

Given the obvious fact that the bit flip error rate must be 50% if the bit is caused by source state of $|0\rangle\langle 0| \otimes \rho$ or $\rho \otimes |0\rangle\langle 0|$, we have

$$\xi_{xx} = \langle T_{xx} \rangle_{\mathcal{L}'} - \frac{1}{2}\mathcal{H}. \quad (15)$$

We can therefore regard the upper bound of \bar{e}_{11}^{ph} as functional of \mathcal{H} as

$$\bar{\mathcal{E}}_{11}(\mathcal{H}) = \frac{T_{xx} + \gamma \sqrt{\frac{T_{xx}}{N_{xx}}} - \mathcal{H}/2}{a_1 b_1 S_{11}} \geq \bar{e}_{11}^{ph}. \quad (16)$$

Therefore, we have the following key rate formula as a functional of \mathcal{H}

$$\mathcal{R}(\mathcal{H}) = p_{z_A} p_{z_B} \cdot \{a_1'' z b_1'' z \underline{S}_{11}(\mathcal{H}) [1 - H(\bar{\mathcal{E}}_{11}(\mathcal{H})) - f S_{zz} H(E_{zz})]\}, \quad (17)$$

where f is the error correction inefficiency and E_{zz} is the observed bit error rate for source zz . The final key is simply the worst-case result of $\mathcal{R}(\mathcal{H})$ over all possible values for \mathcal{H} , i.e.

$$R = \min_{\mathcal{H} \in \mathcal{I}} \mathcal{R}(\mathcal{H}). \quad (18)$$

According to Eq.(24), we have $\mathcal{I} = [h - \delta, h + \delta]$ and

$$\begin{aligned} h &= a_0 S_{ox} + a_0 S_{xo} - a_0^2 S_{oo} \\ \delta &= a_0 \gamma \sqrt{\frac{S_{ox} + S_{xo}}{N_{ox}}} - a_0^2 \gamma \sqrt{\frac{S_{oo}}{N_{oo}}} \end{aligned} \quad (19)$$

given the symmetric set-up that satisfies $a_0 = b_0$, $N_{xo} = N_{ox}$. We shall use such a symmetric case in our numerical simulation.

IV. NUMERICAL SIMULATION

In this section, we present some numerical simulations in comparison with the best known prior art results Ref.[38, 39]. We focus on the symmetric case where the two channel transmissions from Alice to UTP and from Bob to UTP are equal. We also assume that the UTP's detectors are identical, i.e., they have the same dark count rates and detection efficiencies, and their detection efficiencies do not depend on the incoming signals. Also, we assume

$$a_k = b_k, a'_k = b'_k, a''_k = b''_k \quad (20)$$

for all k . And $p_{l_A} = p_{r_B}$ for any $l = r$.

We shall estimate what values would be probably observed for the yields and error yields in the normal cases by the linear models as in [5, 21, 29, 37, 38]. We shall assume 2 types of detectors. Experimental conditions and parameters of detectors [23, 44] are listed in Table I. For the second type of detector, we assume 40% detection and 10^{-7} dark count rate, in Fig.(2,3,4). In

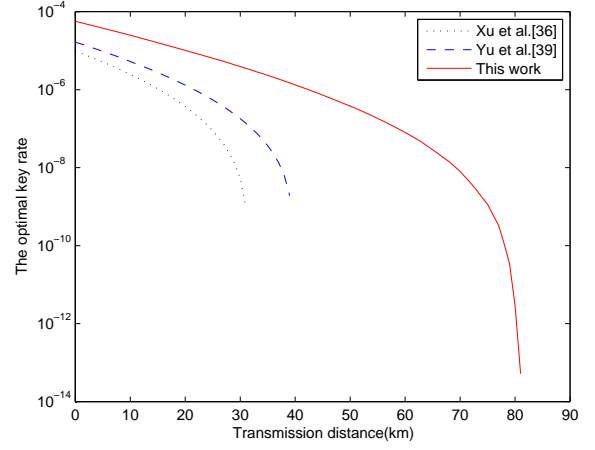


FIG. 1: (Color online) The optimized key rates (per pulse pair) versus transmission distance by different methods with device parameters being given by line a of Table II. Here we set the total number of pulses at each side $N_t = 10^{10}$ and the failure probability $\epsilon = 10^{-7}$.

	e_0	e_d	p_d	η_d	f_e
a	0.5	1.5%	6.02×10^{-6}	14.5%	1.16
b	0.5	1.5%	10^{-7}	40%	1.16
c	0.5	1%	10^{-7}	40%	1.16

TABLE I: Device parameters used in numerical simulations. p_d : the dark count rate. η_d : the detection efficiency of all detectors. f_e : the error correction inefficiency. We shall use the device parameters of line a for the calculation of Fig. 1 and Table II; line b for calculation of Fig. 2, Fig. 3 Fig. 5, Fig. 6, and Table III, and line c for the calculation of Fig. 4.

Fig.(4), we assumed the alignment error probability to be $e_d = 1\%$. With these, the yields and error rate can be simulated [29, 37]. We assume a coherent state for all sources. The density matrix of the coherent state with intensity μ can be written into $\rho = \sum_k \frac{e^{-\mu} \mu^k}{k!} |k\rangle\langle k|$. We calculate the key rate using Eq.(17,18)

A. Numerical results

Here we first take a simple treatment using normal distribution in order to make a fair comparison with the prior art results[38, 39]. This means that we can set $\Delta_+ = \Delta_- = \gamma \sqrt{\frac{S_c}{N_c}}$, and $\gamma = 5.3$ given the failure probability $\epsilon = 10^{-7}$. We emphasize that no matter we use Chernoff bound or the simple treatment, the conclusion that our method can hugely improve the key rates does not change. We use the full parameter optimizations for all protocols [38, 39].

Fig.(1,2,3,4) make a clear view that our method im-

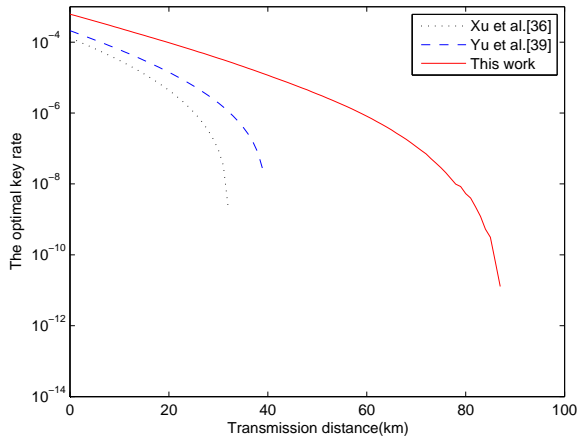


FIG. 2: (Color online) The optimized key rates (per pulse pair) versus transmission distance by different methods with device parameters being given by line *b* of Table I. Here we set the total number of pulses at each side $N_t = 10^9$ and the failure probability $\epsilon = 10^{-7}$.

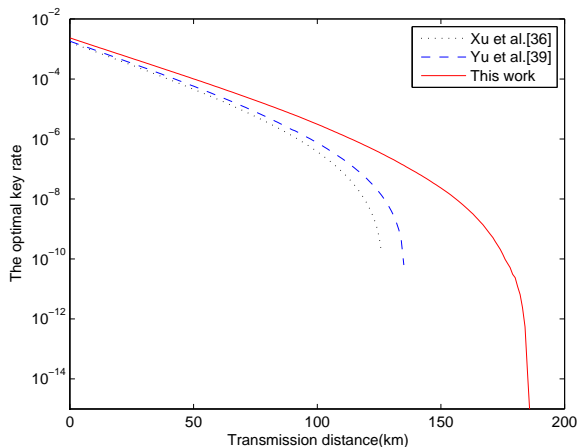


FIG. 3: (Color online) The optimized key rates (per pulse pair) versus transmission distance by different methods with device parameters being given by line *b* of Table I. Here we set the total number of pulses at each side $N_t = 10^{11}$ and the failure probability $\epsilon = 10^{-7}$.

proves the final key rate and transmission distance drastically, and the advantage is much more outstanding when the data size is smaller.

In these figures, the black dotted curve is the key rate obtained from the method in Ref.([38]), where fluctuations of each sources are treated separately. The blue dashed curve is the improved key rate using the method of our previous work in Ref.[39], and the red solid curve is the result of this work.

Table II and Table III list the key rates at different distances for different protocols. From the tables we can see that our method at this work can improve the key

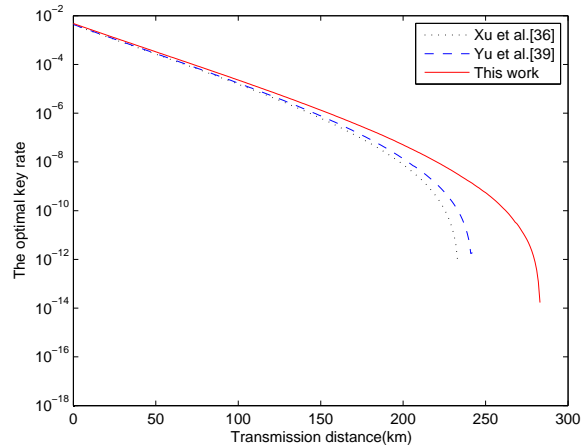


FIG. 4: (Color online) The optimized key rates (per pulse pair) versus transmission distance by different methods with device parameters being given by line *c* of Table I. Here we set the total number of pulses at each side $N_t = 10^{13}$ and the failure probability $\epsilon = 10^{-7}$.

Distance	30 km	35 km	40 km	50 km
Xu et al.[38]	5.32×10^{-9}	-	-	-
Yu et al.[39]	1.81×10^{-7}	3.66×10^{-8}	-	-
This work	3.93×10^{-6}	2.33×10^{-6}	1.33×10^{-6}	3.78×10^{-7}

TABLE II: Comparison of key rates at different distance (standard fiber) for calculations done in Fig.(1).

rate by 20-100 times in a typical parameter set. Table IV lists the optimized parameters of our method at 40 km for our result in Table I and 50 km for our result in Table III.

B. Results with higher security

We have also calculated the key rates by using Chernoff bound[32], the conclusion that our method here can hugely improve the efficiency of MDIQKD keeps unchanged. Consider the Hefei experiment. For a fair comparison, we strictly use Chernoff bound with failure probability 10^{-10} . And also in the final key rate cal-

Distance	35 km	50 km	60 km
Xu et al.[38]	-	-	-
Yu et al.[39]	4.02×10^{-7}	-	-
This work	2.07×10^{-5}	3.44×10^{-6}	8.16×10^{-7}

TABLE III: Comparison of key rate at different distance (standard fiber) for calculations done in Fig.(2).

	μ_x	μ_y	μ_z	p_x	p_y	p_z
II	0.071	0.212	0.280	0.357	0.121	0.479
III	0.078	0.241	0.252	0.398	0.138	0.423

TABLE IV: List of optimized parameters used in numerical simulations by the method of this work. Line II: for 40 km in Table II; Line III: for 50 km in Table III.

culuation, we use the yield lower bound values of those single-photon pairs in Z basis only. Say, we shall replace $\mathcal{S}_{11}(\mathcal{H})$ and $\bar{\mathcal{E}}_{11}(\mathcal{H})$ in Eq.(17) by $\kappa_s \mathcal{S}_{11}(\mathcal{H})$ and $\kappa_e (\bar{\mathcal{E}}_{11}(\mathcal{H}))$, respectively, where the factors κ_s , κ_e are in ranges around 1 due to the possible fluctuations between all single-photon pulses and those from zz source, for the quantities yield and phase-flip error rate, respectively. We use results of Ref.[28] for bounds of κ_s , κ_e .

Also, according to the observed data there[28], we used a linear loss model to estimate the actual over all loss in the experiment. Assuming the same device parameter, we make the optimization by using our 4-intensity protocol. We obtain a final key rate of 0.98 bit per second (bps), which is more than 50 times higher than the reported experimental result, 0.0177 bps.

Furthermore, consider the possibility fresh key application by our method. The standard of GSM requests a transmission rate in 13 kbps. Taking this standard, we calculate the key rates of different protocols with various total number of pulses from 10^9 to 10^{10} , at a fixed distance of 50 km, as shown in Fig.(5). From this figure we can see that our protocol can fulfill the task of private mobile phone communication with only less than 5.9 seconds delay if the system repetition rate is 1 GHz [45]. This is an impossible job for all prior art protocols. For a comparison, we also did the same calculation by Normal distribution approximation as used earlier, with the failure probability 10^{-10} , in Fig.(6). Here, we find the delay time of our protocol is only about 4.1 seconds if the system repetition rate is 1 GHz.

V. CONCLUDING REMARK

In real set-ups of MDI-QKD, the effects of statistical fluctuations caused by the finite-size key must be considered. In the statistical analysis, earlier works[32, 38, 39] used the simple worst-case calculation for single-photon yield and the phase-flip error rate separately, leaving the problem of difference between the error rate in X basis and the phase-flip error in Z basis. Here we used the more economic worse-case estimation pointing directly to the final key rate, and calculate the yield and phase-flip error rate directly Z -basis using the data in X -basis only. These improved the key rate drastically. Also, here in our protocol intensities of pulses at different bases can be different, this further improves the key rate. Also, we have shown that actually both the yield and the phase-

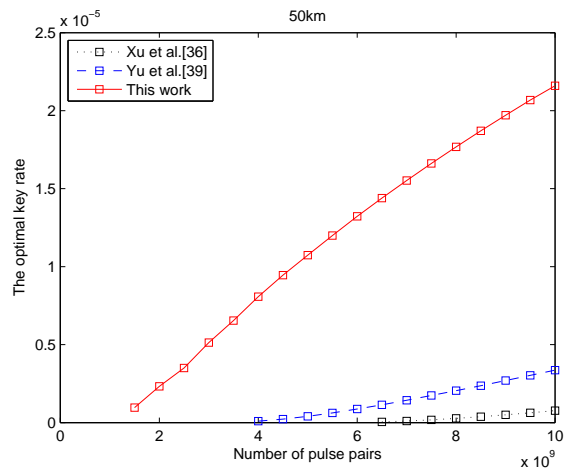


FIG. 5: (Color online) The optimized key rates (per pulse pair) versus different total number of pulse pairs N_t for each protocols at the distance of 50 km. Here the failure probability is $\epsilon = 10^{-10}$, with the device parameters being listed in line b of Table I. We strictly use Chernoff bound in the calculation.

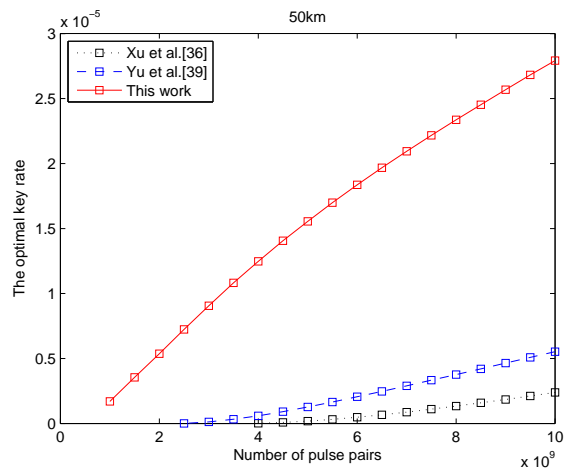


FIG. 6: (Color online) The optimized key rates (per pulse pair) versus different total number of pulse pairs N_t for each protocols at the distance of 50 km calculated by the Normal distribution approximation. Here the failure probability is also set to be 10^{-10} , with the device parameters being listed in line b of Table I.

flip error rate of single-photon pairs can be calculated directly for *all* single-photon pairs using observed data in X basis only. As shown in the numerical simulations, the results obtained with our improved methods are much better than the results obtained before. In short, we have proposed a method that is much more efficient than all known methods for improving key rate in the decoy-state MDI-QKD. Our method has actually made the decoy-state MDI-QKD immediately useful in practice.

In our calculation, we have chosen a special of sources for \mathcal{D} in Eq.(7). As was pointed out already, there are

other choices, e.g., $\{oo, ox, xo, oy, yo, xx, xy, yx\}$ [39], linear programming and so on. The method here can also be applied to the traditional decoy-state BB84 protocol, say Alice has vacuum source, source x, y in X basis and source z in Z basis as the signal source. They use vacuum source and sources x, y to calculate the single photon yield and phase-flip error rate and use source z for key distillation. And also one can treat the single photon yield and phase-flip error rate jointly, taking the optimization directly pointing to the final key rate. This will be reported elsewhere.

Acknowledgement XBW proposed this work and presented key-rate analysis. YHZ and ZWY did the numerical test. YHZ and XBW wrote the paper. We acknowledge the financial support in part by the 10000-Plan of Shandong province (Taishan Scholars), National High-Tech Program of China grant No. 2011AA010800 and 2011AA010803, NSFC grant No. 11474182, 11174177

and 60725416, and the key R&D Plan Project of Shandong Province, grant No. 2015GGX101035.

Note added: Several months after we announced this work in arXiv 1502:01262 (2015), our method proposed in this work has been experimentally implemented very recently[46]. There, 1 GHz source repetition rate is demonstrated with pulses' coherence length of 0.035 ns.

VI. APPENDIX

Given set $\mathcal{L} = \mathcal{D}$, using constraints

$$\langle S_{lr} \rangle_{\mathcal{L}} = \sum_{m,n} c_{mn}^{lr} s_{mn}^{\mathcal{L}}. \quad (21)$$

as shown in Eq.(10), we have

$$s_{11}^{\mathcal{L}} \geq \underline{s}_{11}^{\mathcal{L}} = \frac{[a_1' b_2' \langle S_{xx} \rangle_{\mathcal{L}} + a_1 b_2 a_0' \langle S_{oy} \rangle_{\mathcal{L}} + a_1 b_2 b_0' \langle S_{yo} \rangle_{\mathcal{L}}] - [a_1 b_2 \langle S_{yy} \rangle_{\mathcal{L}} + a_1 b_2 a_0' b_0' \langle S_{oo} \rangle_{\mathcal{L}}] - a_1' b_2' \mathcal{H}}{a_1 a_1' (b_1 b_2' - b_1' b_2)}, \quad (22)$$

$$\text{and } \mathcal{H} = a_0 \langle S_{ox} \rangle_{\mathcal{L}} + b_0 \langle S_{xo} \rangle_{\mathcal{L}} - a_0 b_0 \langle S_{oo} \rangle_{\mathcal{L}}.$$

Since quantities $\langle S_{lr} \rangle_{\mathcal{L}}$ are not exactly determined, we can only find out the lower bound for $\underline{s}_{11}^{\mathcal{L}}$ with constraints for fluctuations given by Eq.(5) in our theorem 1. We can rewrite \mathcal{L} in $\mathcal{L} = \{\mathcal{L}_{mn} | m = 0, 1, 2, \dots; n = 0, 1, 2, \dots\}$ where the subset \mathcal{L}_{mn} (\mathcal{L}'_{mn}) is for all pulse pairs in state $|m\rangle\langle m| \otimes |n\rangle\langle n|$ from set \mathcal{L} (\mathcal{M}). We immediately find that for any source $lr \in \mathcal{D}$, $\mathcal{C}_{mn}^{lr} \in \mathcal{L}_{mn}$

and also $\mathcal{C}_{mn}^{lr} \in \mathcal{L}_{mn}$. Regarding each \mathcal{C}_{mn}^{lr} as \mathcal{M} and $\{\mathcal{C}_{mn}^{lr}\}$ as $\{\mathcal{M}_i\}$ in our theorem, we find that condition 1 in theorem 1 holds. Moreover, one can easily find that all conditions in our theorem 1 hold for sets $\{\mathcal{C}^{lr}, \mathcal{L}\}$ above. Therefore we can use Eq.(5) for constraints of fluctuations. We shall use the following constraints:

$$\begin{aligned} N_{lr} S_{lr} + \gamma \sqrt{N_{lr} S_{lr}} &\geq N_{lr} \langle S_{lr} \rangle_{\mathcal{L}} \geq N_{lr} S_{lr} - \gamma \sqrt{N_{lr} S_{lr}}; \text{ for any } lr \in \mathcal{D} \\ N_{yo} \langle S_{yo} \rangle_{\mathcal{L}} + N_{oy} \langle S_{oy} \rangle_{\mathcal{L}} &\geq N_{yo} S_{yo} + N_{oy} S_{oy} - \gamma \sqrt{N_{yo} S_{yo} + N_{oy} S_{oy}} \\ N_{xx} \langle S_{xx} \rangle_{\mathcal{L}} + N_{yo} \langle S_{yo} \rangle_{\mathcal{L}} + N_{oy} \langle S_{oy} \rangle_{\mathcal{L}} &\geq N_{xx} S_{xx} + N_{yo} S_{yo} + N_{oy} S_{oy} - \gamma \sqrt{N_{xx} S_{xx} + N_{yo} S_{yo} + N_{oy} S_{oy}} \\ N_{yy} \langle S_{yy} \rangle_{\mathcal{L}} + N_{oo} \langle S_{oo} \rangle_{\mathcal{L}} &\leq N_{yy} S_{yy} + N_{oo} S_{oo} + \gamma \sqrt{N_{yy} S_{yy} + N_{oo} S_{oo}} \end{aligned} \quad (23)$$

and

$$N_{ox} S_{ox} + N_{xo} S_{xo} + \gamma \sqrt{N_{ox} S_{ox} + N_{xo} S_{xo}} \geq N_{xo} \langle S_{xo} \rangle_{\mathcal{L}} + N_{ox} \langle S_{ox} \rangle_{\mathcal{L}} \geq N_{ox} S_{ox} + N_{xo} S_{xo} - \gamma \sqrt{N_{ox} S_{ox} + N_{xo} S_{xo}} \quad (24)$$

The first line of Eq.(23) gives individual ranges of statistical fluctuations related to each separate sources, the other lines are *joint* constraints among different sources, as was studied in detail in Ref.([39]).

Second, we use set

$$\mathcal{L}' = \mathcal{D} \cup \mathcal{C}_{11}^{zz}. \quad (25)$$

and quantities

$$\langle S_{lr} \rangle_{\mathcal{L}'} = \sum_{m,n} c_{mn}^{lr} s_{mn}^{\mathcal{L}'}. \quad (26)$$

Note that \mathcal{L}' is simply the set for pulse pairs from sources in \mathcal{D} and single-photon pairs from source zz . As shown in Ref.[22], the states in polarization space for single-photon

pairs in X basis or in Z basis are identical. Both of them are $\frac{1}{4}I$. Similar to the study above for set \mathcal{L} , it is easy to see that all conditions in our theorem 1 hold for sets

$\{\mathcal{L}^{lr}, \mathcal{L}'\}$ above. Similar to Eq.(22), we have the lower bound of $s_{11}^{\mathcal{L}'}$ by

$$s_{11}^{\mathcal{L}'} \geq \underline{s}_{11}^{\mathcal{L}'} = \frac{[a_1' b_2' \langle S_{xx} \rangle_{\mathcal{L}'} + a_1 b_2 a_0' \langle S_{oy} \rangle_{\mathcal{L}'} + a_1 b_2 b_0' \langle S_{yo} \rangle_{\mathcal{L}'}] - [a_1 b_2 \langle S_{yy} \rangle_{\mathcal{L}'} + a_1 b_2 a_0' b_0' \langle S_{oo} \rangle_{\mathcal{L}'}] - a_1' b_2' \mathcal{H}'}{a_1 a_1' (b_1 b_2' - b_1' b_2)}, \quad (27)$$

and $\mathcal{H}' = a_0 \langle S_{ox} \rangle_{\mathcal{L}'} + b_0 \langle S_{xo} \rangle_{\mathcal{L}'} - a_0 b_0 \langle S_{oo} \rangle_{\mathcal{L}'}$.

And we shall use the following constraints from Eq.(5) in theorem 1:

$$\begin{aligned} N_{lr} S_{lr} + \gamma \sqrt{N_{lr} S_{lr}} &\geq N_{lr} \langle S_{lr} \rangle_{\mathcal{L}'} \geq N_{lr} S_{lr} - \gamma \sqrt{N_{lr} S_{lr}}; \text{ for any } lr \in \mathcal{D} \\ N_{yo} \langle S_{yo} \rangle_{\mathcal{L}'} + N_{oy} \langle S_{oy} \rangle_{\mathcal{L}'} &\geq N_{yo} S_{yo} + N_{oy} S_{oy} - \gamma \sqrt{N_{yo} S_{yo} + N_{oy} S_{oy}} \\ N_{xx} \langle S_{xx} \rangle_{\mathcal{L}'} + N_{yo} \langle S_{yo} \rangle_{\mathcal{L}'} + N_{oy} \langle S_{oy} \rangle_{\mathcal{L}'} &\geq N_{xx} S_{xx} + N_{yo} S_{yo} + N_{oy} S_{oy} - \gamma \sqrt{N_{xx} S_{xx} + N_{yo} S_{yo} + N_{oy} S_{oy}} \\ N_{yy} \langle S_{yy} \rangle_{\mathcal{L}'} + N_{oo} \langle S_{oo} \rangle_{\mathcal{L}'} &\leq N_{yy} S_{yy} + N_{oo} S_{oo} + \gamma \sqrt{N_{yy} S_{yy} + N_{oo} S_{oo}} \end{aligned} \quad (28)$$

and

$$N_{ox} S_{ox} + N_{xo} S_{xo} + \gamma \sqrt{N_{ox} S_{ox} + N_{xo} S_{xo}} \geq N_{xo} \langle S_{xo} \rangle_{\mathcal{L}'} + N_{ox} \langle S_{ox} \rangle_{\mathcal{L}'} \geq N_{ox} S_{ox} + N_{xo} S_{xo} - \gamma \sqrt{N_{ox} S_{ox} + N_{xo} S_{xo}} \quad (29)$$

Therefore we arrive at the conclusion below:

In the non-asymptotic case, the yield of single-photon pairs in X basis is lower bounded by Eq.(22), and the yield of all single-photon pairs in both X basis and Z basis is lower bounded Eq.(27).

To a good approximation, we can regard the lower bound of $\underline{s}_{11}^{\mathcal{L}'}$ above as the lower bound of the yield of single-photon pairs in Z basis, since in our protocol most of (actually, almost all) single-photon pairs which can cause effective events are produced in Z basis.

Also, compare Eq.(22) and Eq.(27) we find that, the right side of Eq.(27) actually has the same form of the right side of Eq.(22), but with subscripts \mathcal{L} of $\langle S_{lr} \rangle$ and \mathcal{H} in Eq.(22) being replaced by subscripts \mathcal{L}' and \mathcal{H}' . Obviously, according to the definition of \mathcal{L} and \mathcal{L}' , we immediately find that

$$\mathcal{H} = \mathcal{H}'. \quad (30)$$

We shall simply use the notation \mathcal{H} for both of them. Also, we can easily see that, constraints to $\langle S_{lr} \rangle_{\mathcal{L}'}$ listed in Eqs.(28,29) are identical to constraints to $\langle S_{lr} \rangle_{\mathcal{L}}$ as listed in Eqs.(23,24). Therefore, given \mathcal{H} , the lower bound of $\underline{s}_{11}^{\mathcal{L}}$ calculated from Eq.(22) and Eqs.(23,24) must be equal to the lower of $\underline{s}_{11}^{\mathcal{L}'}$ calculated from Eq.(27) and Eqs.(28,29). And hence we can use only *one* functional form $\underline{s}_{11}(\mathcal{H})$ for both the lower bound of $\underline{s}_{11}^{\mathcal{L}}$ and the lower bound of $\underline{s}_{11}^{\mathcal{L}'}$.

Given theorem 2, we can actually deduce the lower bound of yield of all single-photon pairs basis through using the observed data in X basis only, even for the non-asymptotic calculation. *This makes it possible to treat the yield of single-photon pairs and the phase-flip error of single-photon jointly* because both of them are dependent on the same quantity \mathcal{H} . This makes an important part to improve the efficiency of our key rates.

- [1] C.H. Bennett and G. Brassard, in *Proc. of IEEE Int. Conf. on Computers, Systems, and Signal Processing* (IEEE, New York, 1984), pp. 175-179.
 [2] N. Gisin, G. Ribordy, W. Tittel, *et al.*, *Rev. Mod. Phys.* **74**, 145 (2002); N. Gisin and R. Thew, *Nature Photonics*, **1**, 165 (2006); M. Dusek, N. Lütkenhaus, M. Hendrych,

- in *Progress in Optics VVVX*, edited by E. Wolf (Elsevier, 2006); V. Scarani, H. Bechmann-Pasquonucci, N.J. Cerf, *et al.*, *Rev. Mod. Phys.* **81**, 1301 (2009).
 [3] H. Inamori, N. Lütkenhaus, and D. Mayers, *European Physical Journal D*, **41**, 599 (2007), which appeared in the arXiv as quant-ph/0107017; D. Gottesman, H.K. Lo,

- N. Lütkenhaus, *et al.*, *Quantum Inf. Comput.* **4**, 325 (2004).
- [4] W.-Y. Hwang, *Phys. Rev. Lett.* **91**, 057901 (2003).
- [5] X.-B. Wang, *Phys. Rev. Lett.* **94**, 230503 (2005).
- [6] H.-K. Lo, X. Ma, and K. Chen, *Phys. Rev. Lett.* **94**, 230504 (2005).
- [7] X.-B. Wang, *Phys. Rev. A* **72**, 012322 (2005).
- [8] X. Ma, B. Qi, Y. Zhao, and H. K. Lo, *Phys. Rev. A* **72**, 012326 (2005).
- [9] Y. Adachi, T. Yamamoto, M. Koashi, *et al.*, *Phys. Rev. Lett.* **99**, 180503 (2007).
- [10] M. Hayashi, *Phys. Rev. A* **74**, 022307 (2006); *ibid* **76**, 012329 (2007).
- [11] D. Rosenberg, J.W. Harrington, P.R. Rice, *et al.*, *Phys. Rev. Lett.* **98**, 010503 (2007); T. Schmitt-Manderbach, H. Weier, M. Rürst, *et al.*, *Phys. Rev. Lett.* **98**, 010504 (2007); C.-Z. Peng, J. Zhang, D. Yang, *et al.* *Phys. Rev. Lett.* **98**, 010505 (2007); Z.-L. Yuan, A. W. Sharpe, and A. J. Shields, *Appl. Phys. Lett.* **90**, 011118 (2007); A. R. Dixon, Z. L. Yuan, J. F. Dynes, A. W. Sharpe, and A. J. Shields, *Opt. Express* **16**, 18790 (2008). Y. Zhao, B. Qi, X. Ma, *et al.*, *Phys. Rev. Lett.* **96**, 070502 (2006); Y. Zhao, B. Qi, X. Ma, *et al.*, in *Proceedings of IEEE International Symposium on Information Theory, Seattle (IEEE, New York, 2006)*, pp. 2094–2098.
- [12] X.-B. Wang, C.-Z. Peng, J. Zhang, *et al.* *Phys. Rev. A* **77**, 042311 (2008); J.-Z. Hu and X.-B. Wang, *Phys. Rev. A*, **82**, 012331(2010).
- [13] X.-B. Wang, T. Hiroshima, A. Tomita, *et al.*, *Physics Reports* **448**, 1(2007).
- [14] X.-B. Wang, L. Yang, C.-Z. Peng, *et al.*, *New J. Phys.* **11**, 075006 (2009).
- [15] B. Korzh, C. C. W. Lim, R. Houlmann, N. Gisin, M. J. Li, D. Nolan, B. Sanguinetti, R. Thew, and H. Zbinden, Provably secure and practical quantum key distribution over 307km of optical fibre, *Nature Photonics* **9**, 163C168 (2015); 1 Namekata N, Fujii G, Inoue S, Honjo T, *Appl Phys Lett* 2007; **91**: 011112; Yuan ZL, Dixon AR, Dynes JF, Sharpe AW, Shields AJ, *Appl Phys Lett* 2008; **92**: 201104.
- [16] G. Brassard, N. Lütkenhaus, T. Mor, *et al.*, *Phys. Rev. Lett.* **85**, 1330 (2000); N. Lütkenhaus, *Phys. Rev. A* **61**, 052304 (2000); N. Lütkenhaus and M. Jähma, *New J. Phys.* **4**, 44 (2002).
- [17] B. Huttner, N. Imoto, N. Gisin, *et al.*, *Phys. Rev. A* **51**, 1863 (1995); H.P. Yuen, *Quantum Semiclassic. Opt.* **8**, 939 (1996).
- [18] L. Lydersen, V. Makarov, and J. Skaar, *Nature Photonics*, **4**, 686(2010); I. Gerhardt, L. Mai, A. Lamas-Linares, *et al.*, *Nature Commu.* **2**, 349 (2011)
- [19] D. Mayers and A. C.-C. Yao, in *Proceedings of the 39th Annual Symposium on Foundations of Computer Science (FOCS98)* (IEEE Computer Society, Washington, DC, 1998), p. 503; A. Acin, N. Brunner, N. Gisin, *et al.*, *Phys. Rev. Lett.* **98**, 230501 (2007); V. Scarani, and R. Renner, *Phys. Rev. Lett.* **100**, 302008 (2008); V. Scarani, and R. Renner, in *3rd Workshop on Theory of Quantum Computation, Communication and Cryptography (TQC 2008)*, (University of Tokyo, Tokyo 30 JanC1 Feb 2008) See also arXiv:0806.0120
- [20] S.L. Braunstein and S. Pirandola, *Phys. Rev. Lett.* **108**, 130502 (2012).
- [21] H.-K. Lo, M. Curty, and B. Qi, *Phys. Rev. Lett.*, **108**, 130503 (2012), K. Tamaki, H.-K. Lo, C.-H. F. Fung, *et al.*, *Phys. Rev. A*, **85**, 042307 (2012).
- [22] X.-B. Wang, *Phys. Rev. A* **87**, 012320 (2013).
- [23] A. Rubenok, J. A. Slater, P. Chan, *et al.*, *Phys. Rev. Lett.* **111**, 130502 (2013).
- [24] P. Chan, J. A. Slater, I. Lucio-Martinez, *et al.*, arXiv:1204.0738v1.
- [25] Y. Liu, T.-Y. Chen, L.-J. Wang, *et al.*, *Phys. Rev. Lett.* **111**, 130502 (2013)
- [26] T. Ferreira da Silva, D. Vitoreti, G. B. Xavier, *et al.*, *Phys. Rev. A* **88**, 052303 (2013).
- [27] Z. Tang, Z. Liao, F. Xu *et al.*, *Phys. Rev. Lett.* **112**, 190503(2014).
- [28] Yan-Lin Tang, Hua-Lei Yin, Si-Jing Chen, *et al.*, *Phys. Rev. Lett.* **113**, 190501 (2014).
- [29] X. Ma, C.-H. Fred Fung, and M. Razavi, *Phys. Rev. A* **86**, 052305 (2012).
- [30] Q. Wang and X.-B. Wang, *Phys. Rev. A*, **88**, 052332 (2013).
- [31] F. Xu, M. Curty, B. Qi, *et al.*, *Appl. Phys. Lett.* **103**, 061101 (2013).
- [32] M. Curty, F. Xu, W. Cui, *et al.*, arXiv:1307.1081v1.
- [33] Z.-W. Yu, Y.-H. Zhou, and X.-B. Wang, *Phys. Rev. A* **88**, 062339 (2013).
- [34] Z.-W. Yu, Y.-H. Zhou, and X.-B. Wang, arXiv: 1309.0471v1.
- [35] Z.-W. Yu, Y.-H. Zhou, and X.-B. Wang, arXiv: 1309.5886v1.
- [36] Y.-H. Zhou, Z.-W. Yu, and X.-B. Wang, *Phys. Rev. A* **89**, 052325 (2014).
- [37] Q. Wang, and X.-B. Wang, *Scientific Reports*, **4**, 4612(2014).
- [38] F. Xu, H. Xu, and H.-K. Lo, *Phys. Rev. A* **89**, 052333 (2014).
- [39] Z.-W. Yu, Y.-H. Zhou, and X.-B. Wang, *Phys. Rev. A* **91**, 032318 (2015).
- [40] Although the detector repetition has been demonstrated at GHz by many experiments[15], improving the source repetition rate in MDI-QKD is technically challenging. To reach a repetition rate of GHz level, one needs to realize the interference of independent pulses with a coherence length of fewer than 1 ns. However, it seems that there is no barrier *in principle*.
- [41] There are other choices for set \mathcal{L} . For example, we can choose all pulses given by source x, y, o i.e., $\mathcal{L} = \{oo, ox, xo, oy, yo, xx, yy, xy, yx\}$ and then use linear programming. Here we take such a specific choice in order to show the main idea clearly with explicit formulas which can also make the calculation more efficiently. Cautions should be taken that the computer can present wrong, insecure results quite often if linear programming is used.
- [42] H.-K. Lo and H. F. Chau, *Science* **283**, 2050C2056 (1999).
- [43] D. Gottesman and J. Preskill, *Phys.Rev. A* **63** (2001) 022309.
- [44] R. Ursin, F. Tiefenbacher, T. Schmitt-Manderbach, *et al.*, *Nat. Phys.* **3**, 481 (2007).
- [45] In the calculation, given a system repetition rate of 1 GHz, a key rate of 10^{-9} bit per pulse pair corresponds to a key rate of 1k bps.
- [46] L. C. Comandar, M. Lucamarini, B. Frohlich, J. F. Dynes, A. W. Sharpe, S. Tam, Z. L. Yuan, R. V. Penty, A. J. Shields, arXiv:1509.08137